Acta Pharmaceutica Sinica B 2021;11(9):2900–2913

Chinese Pharmaceutical Association
Institute of Materia Medica, Chinese Academy of Medical Sciences

Acta Pharmaceutica Sinica B

www.elsevier.com/locate/apsb
www.sciencedirect.com

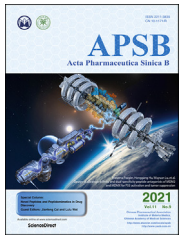

ORIGINAL ARTICLE

Design, synthesis, and biological evaluation of multiple targeting antimalarials

Yiqing Yang[a,†], Tongke Tang[b,c,†], Xiaolu Li[d,†], Thomas Michel[e], Liqin Ling[f,g], Zhenghui Huang[b,h], Maruthi Mulaka[f], Yue Wu[a], Hongying Gao[a], Liguo Wang[a], Jing Zhou[g], Brigitte Meunier[e], Hangjun Ke[f], Lubin Jiang[b,h,*], Yu Rao[a,*]

[a]*MOE Key Laboratory of Protein Sciences, School of Pharmaceutical Sciences, MOE Key Laboratory of Bioorganic Phosphorus Chemistry & Chemical Biology, Tsinghua University, Beijing 100084, China*
[b]*Unit of Human Parasite Molecular and Cell Biology, Key Laboratory of Molecular Virology and Immunology, Institut Pasteur of Shanghai, University of Chinese Academy of Sciences, Chinese Academy of Sciences, Shanghai 200031, China*
[c]*School of Life Science and Technology, ShanghaiTech University, Shanghai 201210, China*
[d]*Department of Biochemistry and Molecular Biology, State Key Laboratory of Medical Molecular Biology, Institute of Basic Medical Sciences, Chinese Academy of Medical Sciences, Peking Union Medical College, Beijing 100005, China*
[e]*Institute for Integrative Biology of the Cell (I2BC), CEA, CNRS, Université Paris-Saclay, Gif-sur-Yvette 91198, France*
[f]*Center for Molecular Parasitology, Department of Microbiology and Immunology, Drexel University College of Medicine, Philadelphia, PA 19129, USA*
[g]*Department of Laboratory Medicine, West China Hospital, Sichuan University, Chengdu 610041, China*
[h]*The Nanjing Unicorn Academy of Innovation, Institut Pasteur of Shanghai, Chinese Academy of Sciences, Nanjing 211135, China*

Received 11 December 2020; received in revised form 11 March 2021; accepted 30 March 2021

KEY WORDS

Drug design;
Multiple targeting compounds;

Abstract Malaria still threatens global health seriously today. While the current discoveries of antimalarials are almost totally focused on single mode-of-action inhibitors, multi-targeting inhibitors are highly desired to overcome the increasingly serious drug resistance. Here, we performed a structure-based drug design on mitochondrial respiratory chain of *Plasmodium falciparum* and identified an extremely potent molecule, RYL-581, which binds to multiple protein binding sites of *P. falciparum* simultaneously

*Corresponding authors. Tel./fax: +86 10 62782025 (Yu Rao), +86 21 54923072 (Lubin Jiang).
E-mail addresses: lbjiang@ips.ac.cn (Lubin Jiang), yrao@tsinghua.edu.cn (Yu Rao).
†These authors made equal contributions to this work.
Peer review under responsibility of Chinese Pharmaceutical Association and Institute of Materia Medica, Chinese Academy of Medical Sciences.

https://doi.org/10.1016/j.apsb.2021.05.008

Antimalarial inhibitors;
Mechanism of action;
Membrane proteins

(allosteric site of type II NADH dehydrogenase, Q_o and Q_i sites of cytochrome bc_1). Antimalarials with such multiple targeting mechanism of action have never been reported before. RYL-581 kills various drug-resistant strains *in vitro* and shows good solubility as well as *in vivo* activity. This structure-based strategy for designing RYL-581 from starting compound may be helpful for other medicinal chemistry projects in the future, especially for drug discovery on membrane-associated targets.

1. Introduction

Malaria remains a major challenge to global health with 50% of the world population at the risk of infection. Today it still causes 229 million new clinical cases and more than 0.4 million deaths annually[1]. Although antimalarial drugs mitigated the epidemics successfully in the past few decades, clinical evidences on resistance for all commercial antimalarial medicines including quinine, chloroquine, atovaquone and artemisinins have been reported[2,3]. To address this issue, and in the absence of a licensed vaccine, developing new type of molecules against the drug-resistant *Plasmodium falciparum* is crucial as resistance to front-line antimalarial drugs (artemisinin-combination therapies, ACTs) is spreading in Southeast Asia and Africa[4,5].

In our continuous studies of developing new antimalarials and investigations of the rational drug design for membrane-associated targets, we pay particular attentions on mitochondrial respiratory chain of *P. falciparum* which is the major pathogenic parasite causing malaria[1,6,7]. Among various antimalarial targets, the respiratory chain of mitochondrial inner membrane of *P. falciparum* (Fig. 1) presents highly attractive target for the development of novel antimalarial drugs, but most of them are mono-targeting inhibitors[6,7]. The parasite encodes five membrane dehydrogenases, namely type II NADH dehydrogenase (NDH2), malate quinone oxidoreductase (MQO), dihydroorotate dehydrogenase (DHODH), glycerol 3-phosphate dehydrogenase (G3PDH), and succinate dehydrogenase (SDH) for generating ubiquinol (QH_2). QH_2 in turn is re-oxidized back to ubiquinone (Q or UQ) by complex III which is needed for maintaining the dehydrogenases activities[7,8]. Complex III and subsequent complex IV activities are required for proton gradient formation, which drives the synthesis of ATP by complex V (Fig. 1). The respiratory chains of *P. falciparum* and human have notable differences. The single-subunit NDH2 of *P. falciparum* (*Pf*NDH2) forms a homodimer and acts as an alternative to the multi-subunit complex I of human[9,10]. In the previous studies[10], we identified RYL-552 as a *Pf*NDH2 inhibitor (Fig. 1) that targets two allosteric pockets and reduces the binding affinity of the substrate NADH. In the cocrystal structure, one of the allosteric pockets localizes at the homodimer interface above the membrane (Supporting Information Fig. S1 and pocket I in Fig. 1) and the other is buried inside the membrane (Fig. S1 and pocket II in Fig. 1). The other substrate

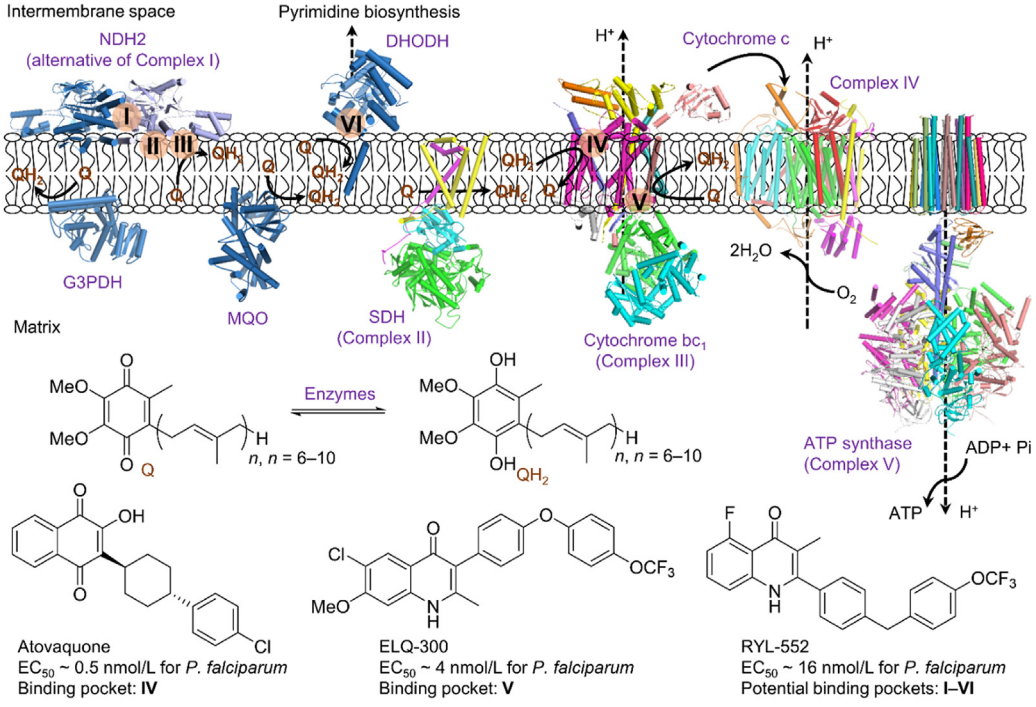

Figure 1 Mitochondrial respiratory chain of *P. falciparum* and its inhibitors. The boldface Roman numerals I–VI present six binding pockets of inhibitors. Pocket I: an allosteric site of *Pf*NDH2, pocket II: the other allosteric site of *Pf*NDH2, pocket III: Q site of *Pf*NDH2, pocket IV: Q_o site of *Pf*bc_1, pocket V: Q_i site of *Pf*bc_1, pocket VI: Q site of *Pf*DHODH.

UQ (or Q) binds to *Pf*NDH2 at a Q site near the membrane (Fig. S1 and pocket III in Fig. 1). A recent work suggested that RYL-552 may bind at Q site of *Pf*NDH2; however, direct experimental evidence was missing[11]. Complex III (or bc_1) is central to mitochondrial function and possesses two Q binding sites, Q_o (pocket IV in Fig. 1) and Q_i (pocket V in Fig. 1), for the oxidation of ubiquinol and the reduction of ubiquinone respectively. It is a validated antimalarial target as shown by the successful development of atovaquone (Fig. 1), a selective Q_o site inhibitor in clinical use for over 20 years, in combination with proguanil[6,7,12]. Unfortunately, the rapid rise of atovaquone resistance caused by mutations at the Q_o site has compromised its use. Interestingly, some genetic evidences suggested that RYL-552 also bound to Q_o site of *Pf*bc_1[13]. Although the Q_i site is more divergent than the Q_o site, target site mutations conferring resistance to the Q_i site inhibitor ELQ-300 (Fig. 1) have been found[14,15]. A compound similar to RYL-552 bound at the Q_i site of *Pf*bc_1 too, but it only very weakly inhibited *Pf*NDH2[16]. In addition to the generation of electrochemical gradient through the respiratory chain, a functional DHODH is also very important for malaria parasites' survival, as DHODH is essential for *de novo* biosynthesis of pyrimidine[8]. The inhibitors of *Pf*DHODH target its Q site (pocket VI in Fig. 1) at the interface with the membrane. One of them, DSM265, is currently in phase-2a clinical trial[17]. Unfortunately, *Pf*DHODH mutations were found in patients' parasites and in some patients, the disease recurred despite DSM265 treatment. *In vitro* selection predicts malaria parasite resistance to *Pf*DHODH inhibitors in a mouse infection model too[18]. Overall, these results highlight the need of developing multi-targeting inhibitors. Our recent studies revealed that RYL-552's analogues inhibited DHODH of human (*Hs*DHODH)[19]. Since *Pf*DHODH and *Hs*DHODH share very similar sequence[20], RYL-552 is likely to weakly target *Pf*DHODH too. Based on these recent data, we presumably thought at the beginning of this project that RYL-552 could be considered as an analogue of Q and thus serve as a promising multi-targeting hit compound by potentially binding to six pockets of three membrane proteins (*Pf*NDH2, *Pf*DHODH and *Pf*bc_1). Although *Pf*NDH2 is dispensable in the asexual blood stages, it's inhibitors can be valuable in mosquito stages for eliminating parasites in mosquito and thus blocking malaria transmission as atovaquone does[21–23]. Design and targets elucidation of multi-targeting inhibitors derived from RYL-552 will provide more powerful antimalarials than mono-targeting inhibitors for both curing symptoms and blocking transmission. On the other hand, as even subtle chemical transformations of the respiratory chain inhibitors can modify the targets selectivity[16,24,25], some unclear results in previous studies need to be further clarified by mapping the inhibitor targets to efficiently guide antimalarial drug development[11].

2. Results and discussions

2.1. Analyzing the six potential binding pockets of RYL-552

To design multi-targeting antimalarials based on RYL-552, we firstly analyzed its potential binding models with all six sites of *Pf*NDH2, *Pf*bc_1 and *Pf*DHODH. The two allosteric sites on *Pf*NDH2 have been elucidated *via* co-crystal structures in our previous study (Fig. 2, pockets I to II)[10]. We then defined the Q site of *Pf*NDH2 from its yeast homologues and docked RYL-552 into it (Fig. 2, pocket III)[26], in which RYL-552 stayed similarly as a previous docking model[11]. Since the structure of *Pf*bc_1 has not been resolved so far, a homology modeling was performed based on its yeast homologue, followed by docking RYL-552 to Q_o and Q_i sites respectively (Supporting Information Fig. S2, Fig. 2 pockets IV and V). In the Q_o site, RYL-552 bound to it *via* an important hydrogen bond with Y268 and π–π stacking with F264 as well as some van der Waals forces, which could reasonably explain the previously observed RYL-552-resistant mutants (F264L, V259L and A122T)[13]. Besides the F264L mutant directly weakened the binding affinity, the other two mutants V259L and A122T could disturb the spatial conformations of Y268 and F264 respectively as their neighboring residues (Fig. 2, pocket IV) and further affect the binding. However, atovaquone-resistant mutant Y268S kept the sensitivity to RYL-552 which could be explained by the structural and binding difference between RYL-552 and atovaquone. In a potential binding model in Y268S Q_o site of *Pf*bc_1 (Supporting Information Fig. S3), RYL-552 inserted into deeper position, while Y268 behaved as a gatekeeper to prevent RYL-552 entering the corresponding position in wildtype. Although RYL-552 lost the binding with Y268, it formed some new interactions in the Y268S mutant including cation–π interaction with K272 and hydrogen bonding with I258 (Fig. S3). In contrast, the carbonyl group in atovaquone, corresponding to the N−H group in the quinolone ring of RYL-552 (Fig. 1), generated steric hindrance with backbone of I258 and couldn't contribute any binding. In the Q_i site (Fig. 2, pocket V), RYL-552 formed hydrogen bonds with Y16, H192 and S196 as well as π–π stacking interactions with F30 and F210. The binding model of RYL-552 in the Q site of *Pf*DHODH was similar with its analogue in *Hs*DHODH[19], containing hydrogen bonds and π–π stacking interactions with R265 and Y168 respectively. Although RYL-552 has been purposed to interact with multiple pockets here, its moderate potency has made the parasites easily generate drug-resistant mutations[13]. These carefully-defined binding models encouraged us to design more potent and drug-like multi-targeting antimalarials from RYL-552.

2.2. Design and synthesis of new antimalarials

We noticed that the quinolone ring of RYL-552 lied inside all pockets, while its trifluoromethyl group was oriented outwards (Fig. 2). First, we introduced hydrophilic groups on the trifluoromethyl group to improve the solubility. After the synthesis and evaluation of several compounds with alternatives to trifluoromethyl group (Fig. 3A, compounds **1**–**6**)[19], we chose compound **6** as a new starting point for further modification because its difluoromethyl group resulted in only a slight loss of the potency. Compounds **7**–**11** were then synthesized, but only compounds **7** and **8** retained some potency. We supposed that the modifications of the molecule moieties outside the binding pockets reduced their binding affinities.

Therefore, we modified the molecule moieties located inside the binding pockets in order to introduce more interactions with binding pockets and enhance the binding affinity in the next (Fig. 3B). According to their shapes and volumes, these six pockets could be roughly divided into two groups. Pockets II, III, and VI are so narrow that there were few possibilities of increasing the binding affinity by decorating RYL-552 (Fig. 2). By contrast, pockets I, IV, and V provided enough space for accommodating additional functional groups in the middle of RYL-552 (Fig. 2). Based on the homologous co-crystal structures of all the four Q sites bound with Q or its analogues (Supporting Information Fig. S4), we hypothesized that the binding affinity could be

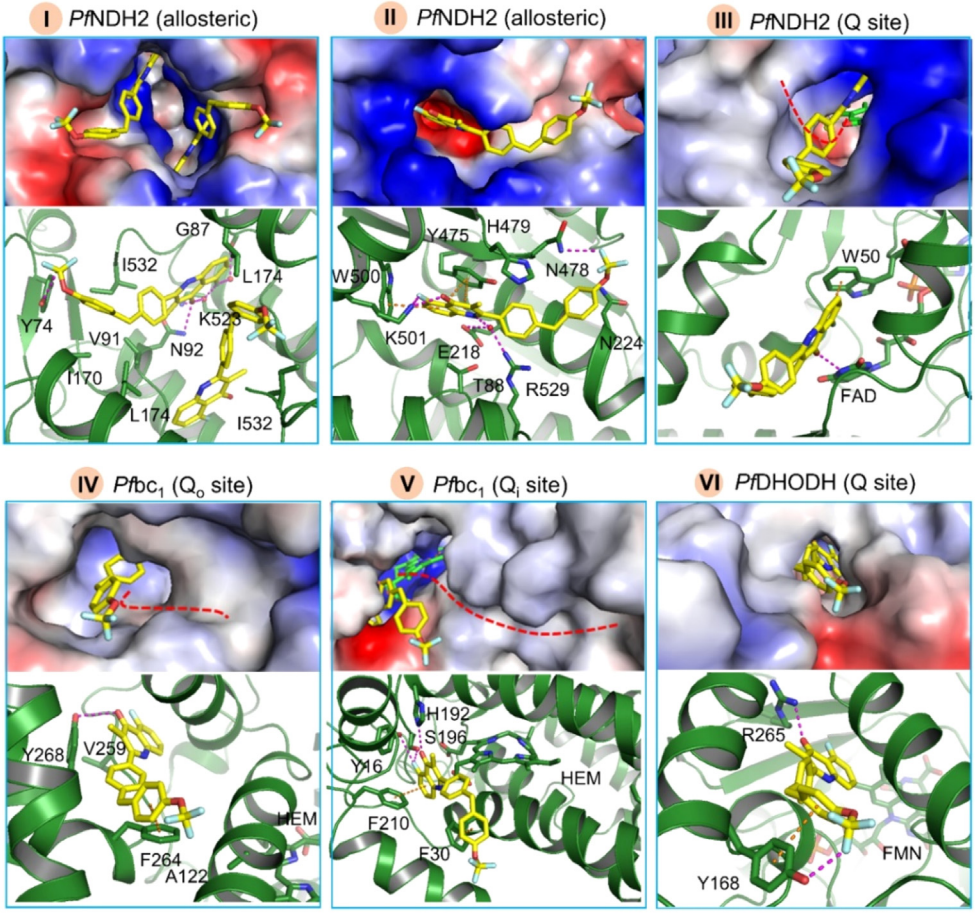

Figure 2 Binding models of RYL-552 with six pockets from *Pf*NDH2, *Pf*DHODH and *Pf*bc$_1$. Binding models in pockets I and II are from a co-crystal structure (PDB code: 5JWC); binding models in pockets III and VI are from *in silico* docking with Q site of *Pf*NDH2 (PDB code: 5JWC) and Q site of *Pf*DHODH (PDB code: 6I4B); binding models in pockets IV and V are from homology modeling with yeast bc_1 (PDB code: 4PD4) and subsequent docking. The red dash lines in pockets III-VI represent the approximate space position of coenzyme Q isoprenyl tail. FAD, flavin adenine dinucleotide; HEM, heme; FMN, flavin mononucleotide. In each pocket, it is presented as surface at the top and cartoon at the bottom.

improved by hybridizing RYL-552 with fragments of Q or its analogues. The HQNO-bound NDH2, the stigmatellin- and UQ_6-bound bc_1, and the UQ_6-bound DHODH from yeast, bacteria and human were aligned with the corresponding binding models of RYL-552 in *Pf*NDH2, *Pf*bc$_1$ and *Pf*DHODH (Fig. S4)[11,12]. In pocket III (Fig. S4B), the hybridization seemed to be difficult because there was no suitable overlap between RYL-552 and HQNO, which was also limited by its small shape as mentioned above. We identified positions on RYL-552 for connecting the long hydrophobic tails of Q analogues in pockets IV–VI (also see the red dash line in corresponding surface picture of Fig. 2). In contrast to the common connecting point on the middle benzene ring of RYL-552 in pockets IV and V, a hybridizing point at the trifluoromethyl group of RYL-552 in pocket VI was more suitable due to its narrow shape and smaller volume (Fig. 2). From our previous study of *Hs*DHODH inhibitors[19], we observed that some larger hydrophobic groups were better than the trifluoromethyl group for inhibiting DHODH activity because the residues around the Q site of DHODH interacted with the membrane and formed a hydrophobic channel for binding Q at the protein−membrane interface (Fig. S4, pocket VI). The strategies for developing inhibitors of the Q site of *Pf*DHODH and of the Q sites in *Pf*bc$_1$ should be obviously different. Besides allowing to target the two Q sites of *Pf*bc$_1$, this hybridization strategy also offered a chance to bind with pocket I at same time, since there was enough space to accommodate functional groups for hybridization in it.

We then mainly focused on the development of multi-targeting inhibitors based on pockets I, IV, and V (Fig. 3B). Encouragingly, compound **12** kept the activity when an ester group was installed on the proposed connecting position (Fig. S4), but more polar carboxylic acid and amide groups altered the compound potency (compounds **13**−**17**). This result supported our hypothesis that some hydrophobic groups should be introduced there to mimic the binding of Q with enzymes. However, their water solubility would become poor if only hydrophobic groups had been added. To balance solubility with hydrophobic interactions, some alkyl-substituted amines were installed on RYL-552 (Fig. 3, compounds **19**−**22**) since compound **18** suggested that a weak dissociative proton was compatible with the activity at that position. On one hand, the alkyl chains could provide hydrophobic interactions as does the long hydrophobic tail of Q; on the other hand, the ionizable aliphatic amine improved the solubility. When a carbon atom in compound **21** was replaced by a hydroxyl group, compound **23** almost lost the potency, indicating again that some hydrophobic groups were required there. Finally, a series of extremely potent antimalarial compounds (compounds **24**−**31**) were identified by further installing a methyl group on the secondary aliphatic nitrogen atom, which could introduce more

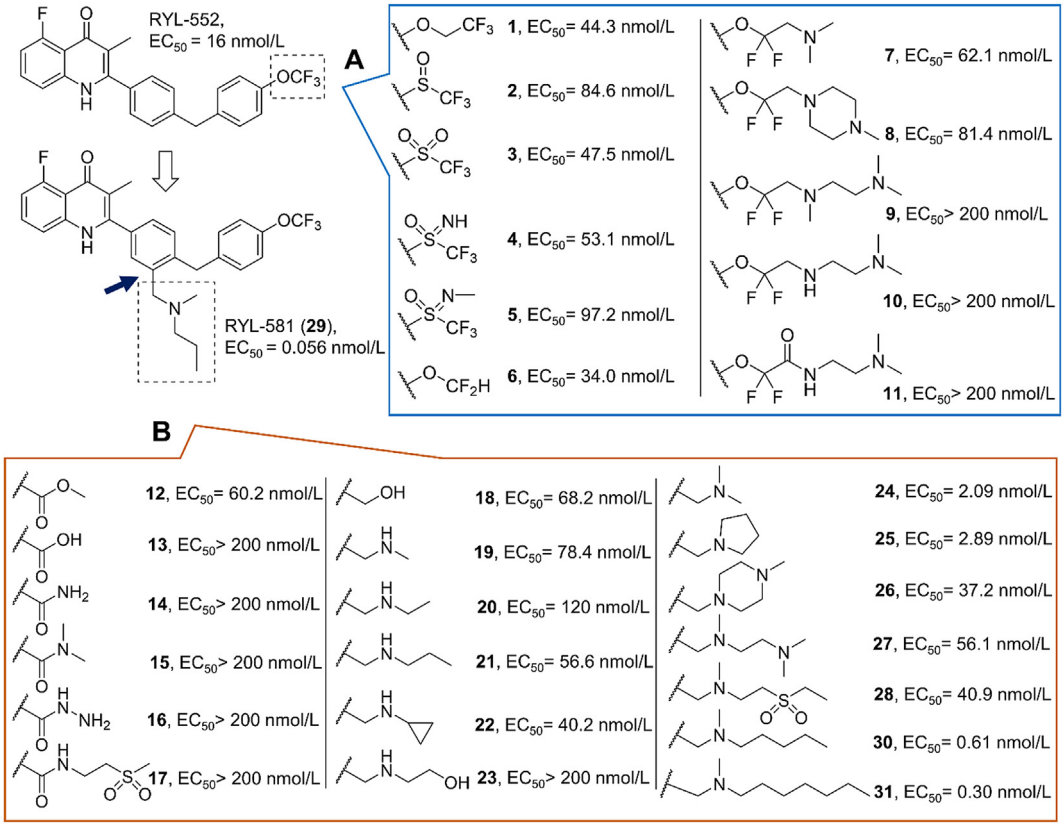

Figure 3 Structure-guided chemical modifications generated the most potent antimalarial RYL-581. (A) Chemical modifications on a position of RYL-552 out the binding pockets. (B) Chemical modifications on a position of RYL-552 in the binding pockets. All the EC_{50} values were means from three replicates on 3D7 strain of *P. falciparum*.

possible hydrophobic interactions and tune their pK_a values[27]. Among them, compound **29** (RYL-581) is an extremely potent antimalarial compound (EC_{50} = 0.056 nmol/L on 3D7 strain). Its potency was improved by near 300-fold as compared to RYL-552, and even significantly better than that of atovaquone (Supporting Information Fig. S5A, EC_{50} = 0.45 nmol/L), which made it stand among the most potent antimalarials for *in vitro* assays. These low EC_{50} values of compounds **24**, **25** and **29**−**31** demonstrated the alkyl chains' contributions to the antimalarial activity. By contrast, compounds **26**−**28** showed less activity because some polar groups such as amines and sulfone, were introduced on the alkyl chains and changed their physicochemical properties.

For the chemical synthesis of designed molecules, compounds **1**−**6** were prepared as before[19]. To prepare compounds **7**−**10** (Scheme 1), the intermediate **32** was generated *via* a phenolic substitution that was followed by the reduction of ester group to obtain compound **33**. After the Miyaura borylation reaction, intermediate **34** was obtained and used as the building block in a Suzuki cross coupling for synthesis of compound **35**. The previous free hydroxyl group in compound **36** was transformed to the leaving group -OTf that was substituted by different amines to generate the intermediates **37**−**40**. Finally, they were condensed with compound **41** to generate the quinolone derivatives as the target compounds **7**−**10**. For the synthesis of compound **11** (Scheme 2), the Suzuki cross coupling reaction was first conducted with compound **42** as the building block to prepare compound **43**. After the hydrolysis, compound **44** was obtained in which the carbonyl group was then protected with ethylene glycol. Compound **45** was used in a phenolic substitution to synthesize compound **46**. After the hydrolysis and deprotection, intermediate **48** was produced and then transformed to an acyl chloride specie, which reacted with amine to build the amide bond in compound **50**. Compound **11** was then obtained as compound **7** in the last synthetic step. For other compounds (Scheme 3), compound **51** was first prepared by a cyanation reaction which was followed by a benzylic bromination *via* radical mechanism. Compound **53** was then synthesized *via* Suzuki cross coupling too. Its ester group was hydrolyzed to carboxylic acid in compound **54** and the cyano group was reduced to aldehyde in compound **55**, which was attacked by Grignard reagent. The secondary alcohol formed and was oxidized to the carbonyl group in compound **58** by Dess-Martin reagent that was utilized for generating compound **12**. Its ester group could be hydrolyzed to carboxylic acid in compound **13** that could be further modified *via* amide condensation to generate compounds **14**, **15** and **17**, or hydrazinolyzed to compound **16**. In addition, it could also be reduced to the hydroxyl group in compound **18** and transformed to aldehyde in compound **59**. Compounds **19**−**31** were finally synthesized *via* reductive amination.

2.3. *Profiles of new antimalarials*

With these promising new compounds in hand, we preliminarily evaluated their drug-like properties. While malaria parasites were significantly inhibited by the compounds (**24**−**25** and **29**−**31**), the cytotoxicity on human liver cells could be rarely observed even at very high concentrations (Table 1, CC_{50} > 10 μmol/L), which

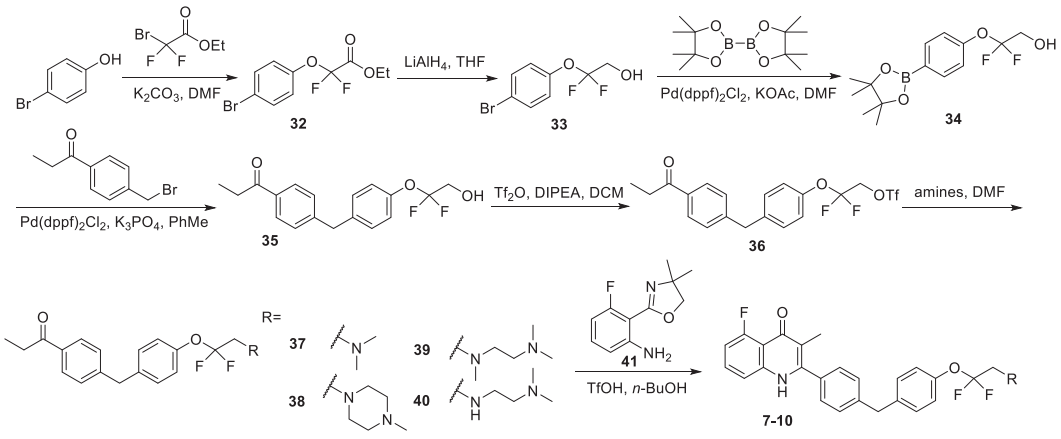

Scheme 1 Synthesis of compounds **7**−**10**.

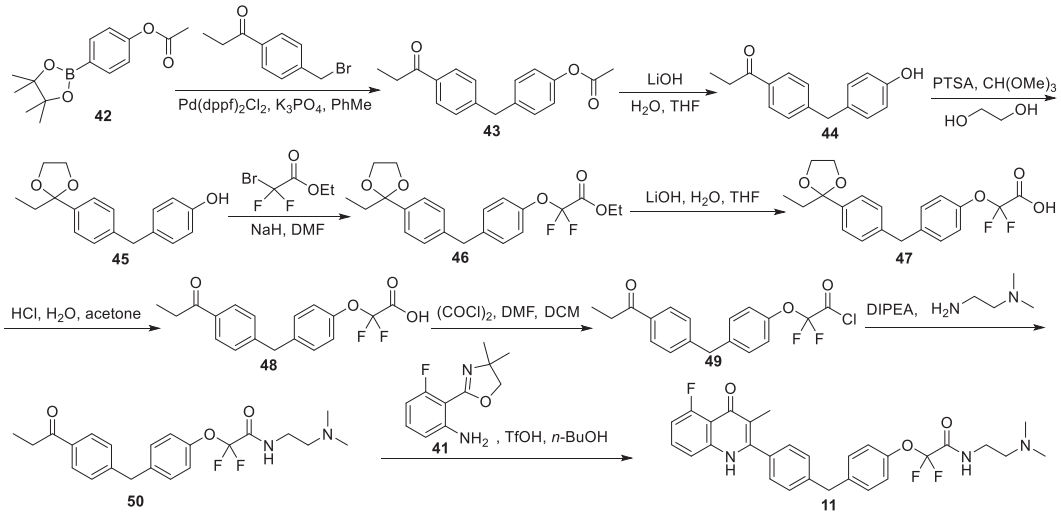

Scheme 2 Synthesis of compound **11**.

indicated their good selectivity indexes (SI). More importantly, the solubility was largely enhanced in various solvents. As shown in Table 1, while RYL-552 was soluble up to 0.27 μmol/L in pure water, the solubility of new compounds has been improved by 8- to 148-fold. In particular, RYL-581 was soluble in water at 13.6 μmol/L. Moreover, these new compounds could be prepared as salt form with their basic aliphatic amine groups to further increase the aqueous solubility. Accordingly, their advantages over RYL-552 and atovaquone were further demonstrated by their higher solubility in a solution of 0.01 mol/L HCl. This was particularly relevant for severe malaria since such patients would not take oral medicine and could be only treated by injection[28]. In contrast, the solubility is low in basic phosphate buffer solution (PBS) like tamoxifen that also contains an aliphatic amine group, and thus a high log*D* value was generated (Supporting Information Table S1). We also observed that the solubility of new compounds in organic phase (Table 1, DCM) was dramatically increased in comparison with RYL-552, which could lead to better distribution in cellular membrane and higher local concentrations near the pockets buried in membrane.

The antimalarial activity of representative new compounds was then evaluated on various *P. falciparum* strains which were identified at different malaria-endemic areas around the world and carried resistance to major clinical antimalarial drugs (Table 2, Fig. S5B–D)[2,10,29]. They potently killed all parasite strains as they did with the 3D7 strain. RYL-581 even displayed sub-nanomolar EC_{50} values in all tests. No correlation of the new compounds with resistance to any specific antimalarial drug was observed, suggesting their different mechanism of action.

To evaluate the new compounds against malaria infection *in vivo*, we observed the outcomes after treatment by RYL-581 on acute *Plasmodium yoelii*-infected mouse models, in which compound RYL-581 was administrated for 4 days at different dosages with chloroquine (CQ) as the positive control (Fig. 4). The blood of infected mice was picked and observed under microscopy to determine the parasitemia during the treatment (Fig. 4A and B). In the DMSO control group, ~30% of erythrocytes were infected after 4 days and all of them were euthanized by Day 7 (Fig. 4C) because they suffered from obvious signs of malarial infection. By contrast, RYL-581 efficiently eliminated the parasites in a dose-dependent manner and only moderate or light infections were observed in the middle of the treatment, though it might be susceptible to metabolism in liver microsomes (Table S1). All mice treated with 10 mg/kg/d RYL-581 were cured by Day 16 and showed 100% survival rate (Fig. 4C), while the parasites could also be completely cleared by Day 22 at a dosage of 3 mg/kg/d RYL-581 under a final

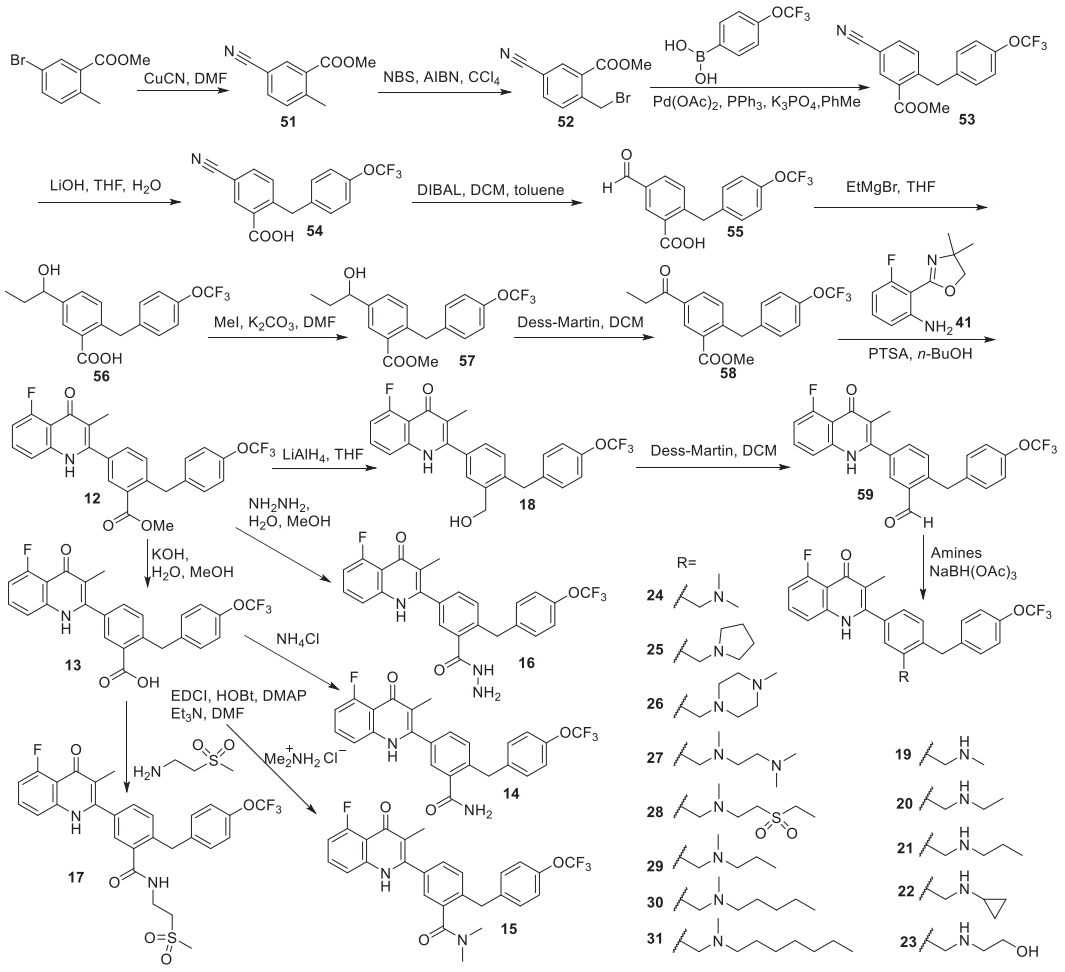

Scheme 3 Synthesis of compounds **12**–**31**.

Table 1 Selectivity index and solubility of new antimalarials.

Compd.	EC_{50} (nmol/L)[a]	CC_{50} (μmol/L)	SI	Solubility (μmol/L)			
				H_2O	0.01 mol/L HCl	MeOH	DCM
Atovaquone	0.45	>10	>22,222	0.7	0.6	2.9×10^4	2.9×10^4
RYL-552	16	>10	>625	0.27	0.68	2.8×10^4	3.3×10^3
24	2.09	>10	>4785	40	496	1.1×10^5	1.9×10^4
25	2.89	>10	>3460	16.3	450	3.7×10^4	3.0×10^4
RYL-581 (**29**)	0.056	>10	>178,571	13.6	428	3.7×10^4	6.4×10^4
30	0.61	>10	>16,393	6.4	337	3.4×10^4	3.7×10^5
31	0.3	>10	>33,333	2.0	19.4	3.2×10^4	4.2×10^5

[a]The values were tested on 3D7 strain. All values were means from three replicates. SI, selectivity index; MeOH, methanol; DCM, dichloromethane.

survival rate of 80%. All the above data suggested that the new compounds had good potential for eliminating malaria *in vivo*.

2.4. *Targets elucidation of RYL-581*

At the beginning, we tried very hard to follow the procedure of resistant selection for targets elucidation in literatures[13,30], but resistant strains were not obtained after many attempts in this case. Therefore, we tested each possible binding site by monitoring the enzymatic activities one by one. First, we used the yDHODH transgenic D10 parasite line (D10attB-yDHOD)[31], which expressed the yeast dihydroorotate dehydrogenase (DHODH) gene of *Saccharomyces cerevisiae*, to confirm the activity of our compounds on the respiratory chain (Fig. 5A)[8,31]. Previous studies have shown that expression of the yDHODH gene could bypass the need for a functional respiratory chain in asexual parasites because yDHODH could replace *Pf*DHODH in the essential pyrimidine biosynthesis pathway[8,31]. Thus, yDHODH transgenic parasites are resistant to antimalarials targeting the mitochondrial respiratory chain including bc_1 inhibitors and *Pf*DHODH inhibitors. As previously shown[8,21], in yDHODH transgenic parasites, a low dose of proguanil could restore sensitivity of inhibitors.

Table 2 New antimalarials killed various drug-resistant *P. falciparum* strains[a].

Strain	Parasites origin	Drug resistance	EC_{50} (nmol/L)		
			24	**25**	RYL-581 (**29**)
803	Cambodia	Dihydroartemisinin (DHA)	9.30	9.81	0.96
Fab9	KwaZulu	None known	6.01	5.33	0.27
C2A	Thailand	Quinine (QN)	1.44	7.01	0.29
GB4	Ghana	Chloroquine (CQ)	1.02	1.41	0.23
CP286	Cambodia	Mefloquine (MQ), sulfadoxine-pyrimethamine (SP)	4.56	4.81	0.27
PC26	Peru	Amodiaquine (AMQ), CQ, QN, SP	3.17	3.30	0.31
Dd2	Indochina	AMQ, CQ, QN, SP	2.05	2.18	0.44
D10	Papua New Guinea	None known	3.23	2.32	0.70

[a]RYL-552 was used as control and showed similar EC_{50} values as before[10]. All the EC_{50} values were means from three replicates.

It has been proposed that mitochondrial membrane potential (Ψ_m) is primarily maintained by mitochondrial electron transport complexes (bc_1 and cytochrome *c* oxidase) but could be also be maintained by the reverse rotation of the F_oF_1 ATP synthase complex when the respiratory chain is chemically inhibited[8]. Proguanil is believed to target F_oF_1 ATP synthase. When tested in combination with proguanil, bc_1 inhibitors are able to kill yDHODH transgenic parasites since both mechanisms for generating Ψ_m are blocked. In contrast, *Pf*DHODH inhibitors fail to kill yDHODH transgenic parasites in the presence of proguanil as the respiratory chain is not inhibited. Thus, we tested our compounds in wildtype (D10 strain) and yDHODH transgenic parasites in the absence and presence of proguanil to determine if our new compounds target *Pf*bc_1.

As expected, yDHODH parasites were highly resistant to RYL-552 and RYL-581, while the sensitivity to these compounds was regained upon proguanil treatment (Fig. 5A). Thus, RYL-552 and RYL-581 acted against the yDHODH parasites through a mechanism similar to that of atovaquone, indicating that RYL-552 and RYL-581 mainly targeted the mitochondrial respiratory chain (Fig. 5A). The compounds were also tested with our in-house recombinant *Hs*DHODH[19]. We only observed a weak inhibition by RYL-552 (Supporting Information Fig. S6A, IC_{50} = 3.0

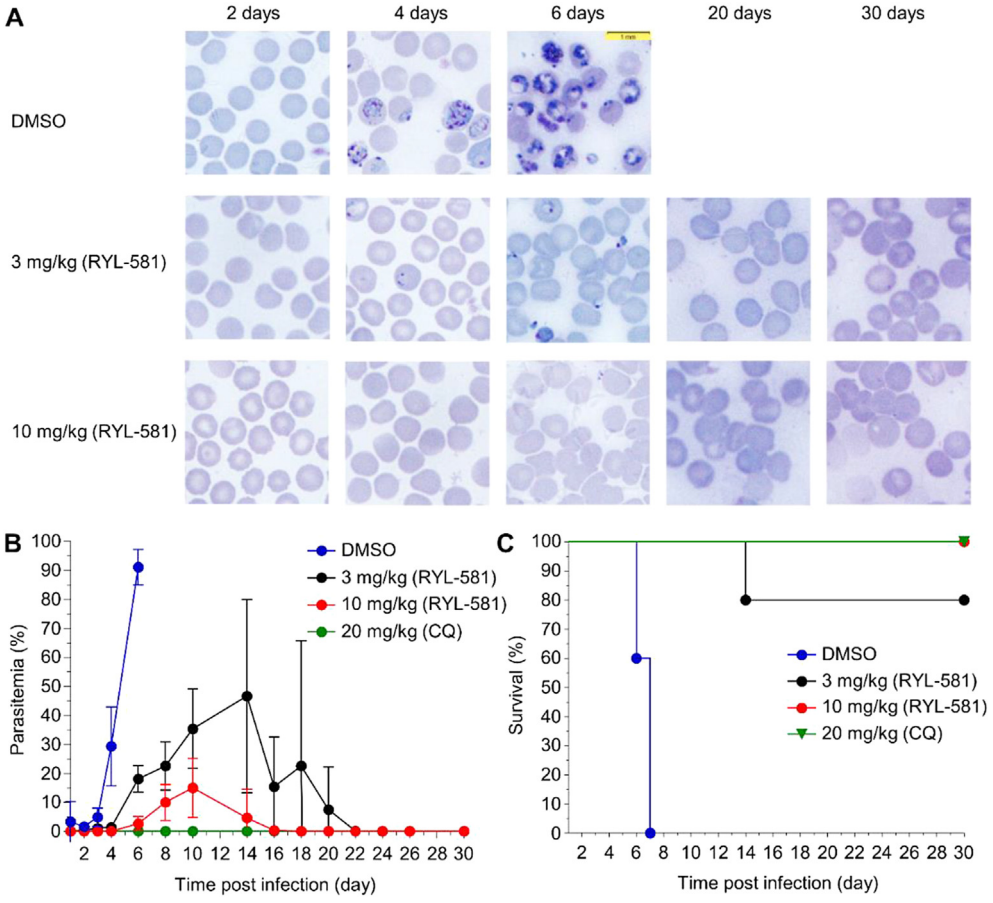

Figure 4 *In vivo* studies of RYL-581 on *P. yoelii*-infected mice. (A) Microscopy of blood smears from mice. The scale bar represents 1 mm. (B) Overview of parasitemia. Compounds were given to mice on Day 1 after infection. There were 5 mice in each group, which were treated by different intraperitoneal dosages once a day for successive 4 days. (C) Survival curves for different dosages. Chloroquine (CQ) was used as the positive control. Error bars represent standard deviation. Data are presented as mean ± SD (n = 5).

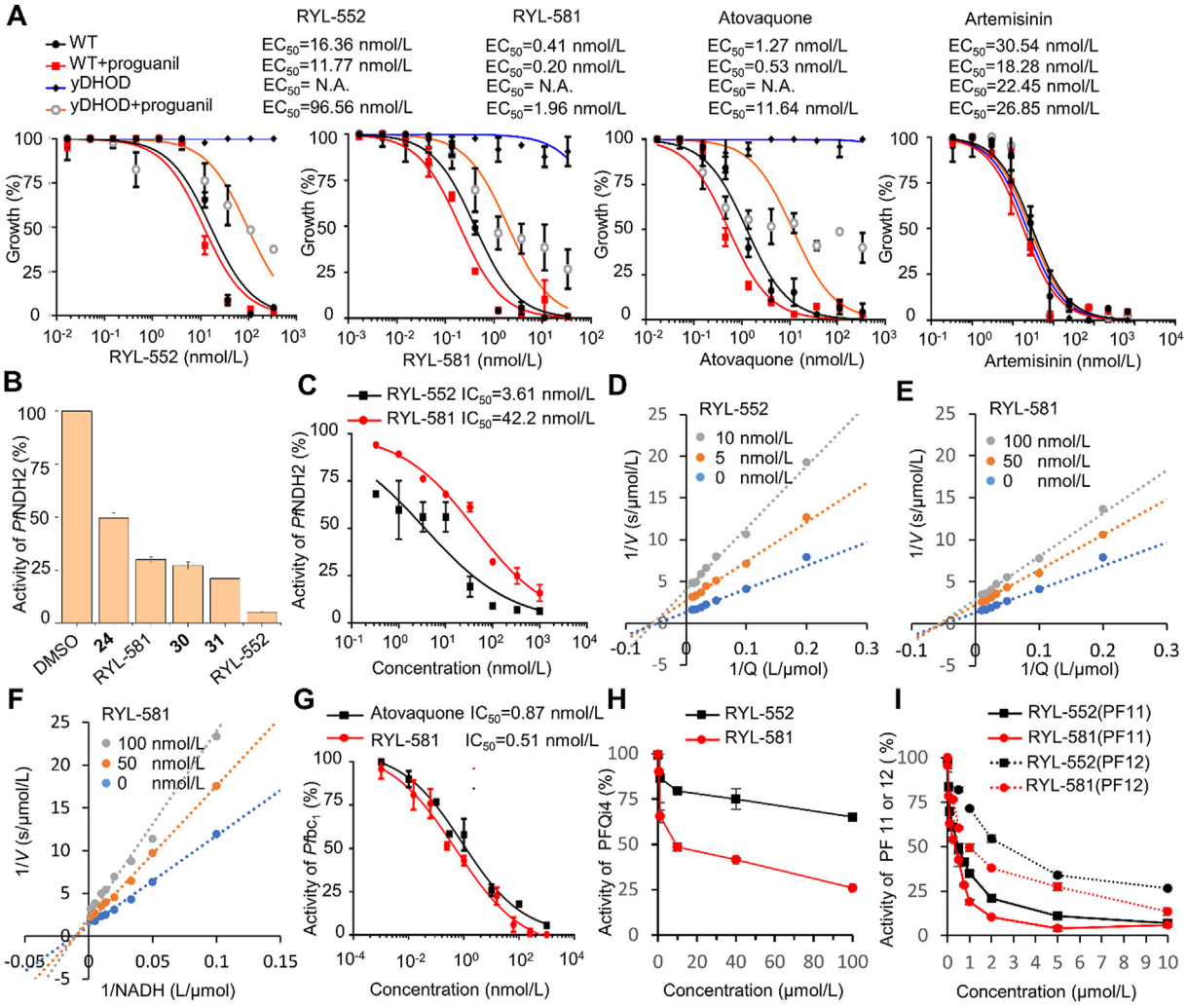

Figure 5 Targets elucidation of RYL-552 and RYL-581. (A) yDHOD transgenic (yDHOD) or wildtype (WT) D10 parasites were challenged with RYL-552, RYL-581, atovaquone and artemisinin in the presence or absence of proguanil (50 nmol/L). Averaged EC_{50} values were shown, which were not available (N.A.) in yDHOD parasites when the parasites were fully resistant to compounds. (B) Inhibition to *Pf*NDH2 by RYL-552 and new compounds at 100 nmol/L. (C) Inhibitory curves of *Pf*NDH2 with RYL-552 and RYL-581. (D) Lineweaver−Burk plot of RYL-552 and Q on *Pf*NDH2. (E) Lineweaver−Burk plot of RYL-581 and Q on *Pf*NDH2. (F) Lineweaver−Burk plot of RYL-552 and NADH on *Pf*NDH2. (G) Inhibition of *Pf*bc_1 by RYL-581 and atovaquone. (H) Inhibition to Q_i site of yeast bc_1 complex with *P. falciparum*-like modifications (PFQi4). The enzyme was, as the WT, fully inhibited by atovaquone at 1 μmol/L. (I) Inhibition to Q_o site of yeast bc_1 complex with *P. falciparum*-like modifications (PF11 or PF12). Data are presented as mean ± SD (n = 3).

μmol/L *vs*. IC_{50} > 10 μmol/L). Because of the very similar structures of *Hs*DHODH and *Pf*DHODH (Fig. S6B), it is likely that only RYL-552 could weakly inhibit *Pf*DHODH. The smaller Q site of *Pf*DHODH would not accommodate the large aliphatic amine groups on the new compounds (Figs. S4B and S6C). As a negative control, artemisinin didn't inhibit the respiratory chain[32,33] and its antimalarial activity was not affected by proguanil in both wild type D10 and yDHODH transgenic parasites (Fig. 5A).

In the following enzymatic activity assays on *Pf*NDH2, our new compounds exhibited stronger inhibition as their alkyl chains lengthened (Fig. 5B), indicating that the designed aliphatic amine groups contributed to the binding affinities. The potency of RYL-581 decreased 11-fold as compared to RYL-552 (Fig. 5C, IC_{50} = 42.2 nmol/L *vs*. IC_{50} = 3.6 nmol/L), which might be resulted from the dual inhibition of two allosteric sites by RYL-552 while RYL-581 might only bind to pocket I. We then checked whether RYL-552 or RYL-581 competitively bound at the Q site of *Pf*NDH2 as proposed in a study on the basis that disordered electron density at the Q site of our previous co-crystal structure could come from RYL-552[10,11]. We thus performed an enzyme kinetic study by measuring substrate−velocity curves in the presence of several concentrations of inhibitors. As shown in the double reciprocal Lineweaver−Burk plot (Fig. 5D), RYL-552 behaved as a non-competitive inhibitor of *Pf*NDH2. This result plus our previous kinetic study with NADH validated its allosteric mechanism again[10]. When the enzyme kinetics were conducted with RYL-581, similar results were observed: K_m values remained unchanged and Vmax values decreased in the presence of RYL-581 for both Q and NADH (Fig. 5E and F). It seems therefore that both RYL-552 and RYL-581 are non-competitive inhibitors and thus unlikely to bind in the Q site of *Pf*NDH2.

For the enzymatic activity of *Pf*bc_1, RYL-581 showed even stronger inhibition than atovaquone (Fig. 5G, IC_{50} = 0.51 nmol/L *vs*. IC_{50} = 0.87 nmol/L), which was consistent with the results in

parasites' growth inhibition assays (Table 1 and Fig. S5A). In order to further confirm their binding sites in *Pf*bc$_1$, we used *P. falciparum*-like yeast *bc*$_1$ mutants with modified Q$_o$- or Q$_i$-site where yeast amino acids were replaced by *P. falciparum* orthologues. Mutant PFQi4 combines 13 amino acid replacements in the Q$_i$-site: Y16H, I17L, S20Y, Q22C, S34F, L40F, V41F, A191L, I195F, L198I, M221F, F225L and I226L. Mutant PF11 harbors ten amino-acid substitutions in the Q$_o$-site, C133V, C134L, V135P, Y136W, H141Y, L275F, R283K, M295V, F296L and I299L (Supporting Information Fig. S7)[34,35]. PF12 carries the same changes as PF11 combined with the atovaquone resistance mutation Y279S. The wildtype yeast *bc*$_1$ complex was found to be highly resistant to RYL-522 and RYL-581, as only slight inhibition was observed at 10 μmol/L (data not shown) while the enzyme was fully inhibited by atovaquone at 1 μmol/L[34], which indicated that our compounds are species-specific. PFQi4 *bc*$_1$ complex with *P. falciparum*-like modifications in the Q$_i$-site showed a slightly lower resistance to RYL-552 and an increased reactivity to RYL-581 (Fig. 5H, IC$_{50}$ ≈ 10 μmol/L) compared to wild type, suggesting that RYL-581 might also display a stronger inhibitory activity towards the Q$_i$ site of *Pf*bc$_1$ than RYL-552. *Pf*bc$_1$ Q sites could be much more sensitive towards our compounds than the mutant yeast sites. A yeast mutant harbouring a fully mutated *P. falciparum*-like Q sites might present an increased sensitivity. Unfortunately, such mutant could not be produced.

PF11 *bc*$_1$ complex with *P. falciparum*-like modifications in the Q$_o$-site clearly presented an increased sensitivity to the compounds (Fig. 5I). The mid-point inhibitory concentrations were around 0.5 μmol/L for RYL-522 and 0.3 μmol/L for RYL-581. Interestingly, the atovaquone-resistant mutation Y279S (Y268S in *P. falciparum*) caused only a modest decrease in sensitivity to RYL-522 and RYL-581 (Fig. 5I, PF11 *vs.* PF12). The mid-point inhibitory concentrations were around 3 μmol/L for RYL-522 and 1 μmol/L for RYL-581, thus a six- and three-fold increase as compared to the values obtained with PF11. This is in sharp contrast to the >100-fold increase in atovaquone mid-point inhibitory concentration obtained with PF12 compared to PF11, as previously observed[35]. As RYL-552 was shown to overcome the atovaquone-resistant mutation Y268S in *P. falciparum*[13], our new compounds are also expected to remain potent in atovaquone-resistant strains in addition to the resistant strains shown in Table 2.

Taken together, the data indicated that RYL-581 simultaneously bound with allosteric site of *Pf*NDH2, Q$_o$ and Q$_i$ sites of *Pf*bc$_1$. This multiple targeting mechanism of action has been never reported for antimalarials before. We then further analyzed the models of RYL-581 binding into Q sites of *Pf*bc$_1$ under membrane-free and membrane-surrounded conditions *via* molecular docking or molecular dynamic (MD) simulation which could mimic the interactions on purified enzyme level and cell level respectively. The binding models of RYL-581 in targeting pockets under membrane-free conditions (Supporting Information Fig. S9A–D) might be different from the models in membrane-surrounded environments. We supposed that the reversibly ionized aliphatic amine chain improved both aqueous solubility and membrane distribution (Table 1), which were helpful for reaching all sites exposed to the aqueous phase or buried in membrane (Fig. S9E). In order to address the question of how the membrane would affect the compounds binding, a molecular dynamic (MD) simulation of 100 ns was performed with the cytochrome *b* of *P. falciparum* in the presence of membrane (Fig. S9F and G). When the system was in equilibrium, we observed that RYL-581 still remained in the two pockets but their conformations clearly shifted under the influence of phospholipids. These computational models indicated that the interactions of RYL-581 with protein and membrane components stabilized its binding at the pockets and ensured its activity.

3. Conclusions

Although enzymes on mitochondrial respiratory chain of *P. falciparum* have been druggable for a long time, their inhibitors, such as atovaquone, ELQ-300 and DSM265 are nearly all single mode-of-action molecules and drug-resistant mutants against them appear[2,6,13,24,30]. Multi-targeting inhibitors may impede the drug resistance. For *Pf*NDH2 inhibitors like CK-2-68 and RYL-552, their detail binding pockets have never been elucidated until our previous work revealed the allosteric mechanism, which provided the basis for rational drug design[9,10]. Although RYL-552 was also proposed to be a competitive inhibitor binding at the Q site of *Pf*NDH2[11], we here provided experimental evidence that both RYL-552 and RYL-581 are non-competitive inhibitors of *Pf*NDH2 (Fig. 5D–F). Compounds like RYL-552 could be viewed as analogues of Q and could possibly target several Q binding sites of enzyme using Q as substrate or co-factor. An extremely potent compound, RYL-581, was then designed based on RYL-552. The compound targets the allosteric site of *Pf*NDH2, and both the Q$_o$ and Q$_i$ sites of *Pf*bc$_1$. Although *Pf*NDH2 seems to be dispensable in the asexual blood stages, its inhibition could be relevant for other stages like mosquito stages[21−23]. Moreover, NDH2 has also been proposed or validated as target for other infectious pathogens including *Mycobacterium tuberculosis*, *Toxoplasma gondi* and *Streptococcus agalactiae*[36−38]. The successful design strategy to build RYL-581 from RYL-552 could be translated to other fields in drug discovery and development. It could even be utilized for further optimizations of atovaquone, ELQ-300 or other analogues. Synergistic effects are usually observed by combination of compounds with different targets, for example, dual inhibition of Q$_o$ and Q$_i$ sites of *Pf*bc$_1$ by combination therapy of atovaquone and ELQ-300 gives better antimalarial effect[15]. The excellent potency of our compounds may also be caused by similar synergistic effects to some extent. In our views, these compounds may have broader pharmacological interactions with Q-related proteins as the kinase inhibitors targeting ATP binding pockets.

It has been suggested that delocalized lipophilic cations (DLCs) tend to accumulate in the mitochondria due to the negatively charged at the matrix site of the membrane[39,40]. Similarly, because of the reversibly ionized aliphatic amine chain, RYL-581 may better reach its mitochondrial targets in response to the proton gradient (Fig. 1). To elucidate the roles of aliphatic amine chains in enhancing activity for *Pf*bc$_1$, some computational models were established (Supporting Information Figs. S8 and S9), in which RYL-581 bind to *Pf*bc$_1$ in membrane-free (Fig. S9A–D) or membrane-surrounded environments (Fig. S9E–G). The binding modes of compounds with proteins could be different in the presence or absence of membrane. The aliphatic amine chain could interact with residues of protein or components of membrane in the protein–membrane interfaces that could be instructive for other drug designs and deserve further investigation in the future.

4. Experimental

4.1. Chemistry

All commercial chemical materials (Energy, Bide, Aladdin, J&K Chemical Co., Ltd.) were used without further purification. All

solvents were analytical grade. The ^{1}H-NMR and ^{13}C-NMR spectra were recorded on a Bruker AVANCE III 400 MHz spectrometer in $CDCl_3$, CD_3OD, or DMSO-d_6 using tetramethylsilane (TMS) or solvent peak as a standard. All ^{13}C-NMR spectra were recorded with complete proton decoupling. Low resolution mass spectral analyses were performed with a Waters ACQUITY UPLCTM/MS. Analytical thin-layer chromatography (TLC) was performed on silica gel 60 F254 plates (Yantai Chemical Industry Research Institute), and flash column chromatography was performed on silica gel 60 (200−300 mesh, Qingdao Haiyang Chemical Co., Ltd.). A BUCHI Rotavapor R-3 was used to remove solvents by evaporation. The purity of the final tested compounds is more than 95% confirmed by NMR and UPLC. In the UPLC analysis, the C18 reverse phase column (Waters ACQUITY) and full-wavelength scanning were used with solvent A (MeCN) and solvent B (0.1% formic acid in H_2O) as the eluent. The ratio of solvent A to solvent B was 1:9 at the beginning and gradually changed to 9:1 at the end. Compounds **16** were synthesized as before[19]. See the synthesis for other compounds and intermediates in Supporting Information.

4.2. Biological materials

P. falciparum parasites were cultured with RPMI 1640 medium (Invitrogen by Thermo Fisher Scientific) supplemented with 5 g/L Albumax I (Invitrogen), 10 mg/L hypoxanthine, 2.1 g/L sodium bicarbonate, HEPES (15 mmol/L), and gentamycin (50 μg/mL). Cultures were maintained in human red blood cells (Type O, Interstate Blood Bank, Tennessee) and kept in a CO_2/O_2 incubator filled with a low oxygen mixture (5% O_2, 5% CO_2, and 90% N_2). Equine cytochrome *c*, decylubiquinone and atovaquone were obtained from Sigma Aldrich. CCK-8 was obtained from YEASEN. The yeast culture media were: YPD (1% yeast extract, 2% peptone and 3% glucose) and YPGal (1% yeast extract, 2% peptone, 0.1% glucose and 2% galactose). Human hepatocarcinoma cells (HepG2) were cultured in DMEM medium supplemented with 10% fetal bovine serum and penicillin-streptomycin. PEGylated castor oil for animal study was purchased from ACROS (Lot: A0377508).

4.3. Parasites growth inhibition assays

For SYBR Green I-based fluorescence assays, asynchronous cultures of *P. falciparum* parasites were pretreated with 0.5 mol/L alanine/10 mmol/L HEPES or 5% sorbitol. Compounds were dissolved in DMSO to make 10 mmol/L stock solutions and diluted serially in 96-well plates. Parasite strains as mentioned in the text (0.5% parasitemia, 2% hematocrit) at the mid-ring stage (∼6−10 h post invasion) were used to test antimalarial efiects. Parasites were incubated in triplicate with pre-diluted compounds and kept for 72 h under an atmosphere of gas mixture containing 5% CO_2, 5% O_2, and 90% N_2 at 37 °C. After 72 h, the plates were frozen at −80 °C overnight and thawed at 37 °C for 1 h. Then 150 μL of lysis buffer (containing SYBR Green I and 20 mmol/L Tris, 5 mmol/L EDTA, 0.008% saponin, 0.08% Triton X-100) was added directly to the wells, followed by gentle mixing and incubation for another 2 h at room temperature in dark. SYBR Green I is from Invitrogen (supplied in 10,000 × concentration). Then the plates were examined for the relative fluorescence units (RFU) per well using the fluorescence plate reader (485 nm excitation and 538 nm emission, Tecan, Infinite F Plex). EC_{50} values were determined by nonlinear regression analysis of logistic concentration (GraphPad Prism software).

4.4. Cytotoxicity assay

HepG2 cells were seeded at a density of 6,000 per well in 96-well plates containing 50 μL medium in each well and incubated at 37 °C in a humidified 5% CO_2 atmosphere. After cultured to attach at 37 °C overnight, another 50 μL medium containing 1 μL compound solutions in DMSO was transferred to each well. The plates were then incubated for additional 24 h. The CCK-8 solution (10 μL for each well) was then added, and the plates were returned to the incubator for 2−4 h. Finally, it was measured at wavelength of 450 nm. EC_{50} values were determined by nonlinear regression analysis of logistic concentration (GraphPad Prism software).

4.5. Measurement of solubility

Solid material was added into a 1.5 mL tube containing solvent to prepare a supersaturated solution. The mixture was incubated for 24 h on a shaker at room temperature, followed by centrifuge and filtration. The supernatant was transferred to another tube. For the aqueous solvent, the concentration was analyzed by a reversed phase HPLC under a pre-calculated standard curve, which was generated by a series of diluted concentrations in methanol. For the organic solvent, the remained solid was directly weighted after removing under reduced pressure.

4.6. In vivo efficacy study

Five BALB/c female mice (25 g, 6−8 weeks) in each group were kept in specific pathogen-free conditions and fed *ad libitum*. Compounds were dissolved in aqueous solution containing DMSO 5% and PEGylated castor oil 18%. Mice were infected by intraperitoneal injection with about 1×10^6 infected red blood cells (Day 0), randomized, and divided into groups of five mice for each compound. Parasitemia were determined by microscopic examination of Giemsa-stained blood smears taken from mice. Intraperitoneal injection of antimalarial compounds was performed as pointed in the result. The mice were euthanized by CO_2 when they had obvious signs of pain, distress or torment. The use of laboratory animals was reviewed and approved by the Ethical Committee of Institut Pasteur of Shanghai, Chinese Academy of Sciences (IACUC issue NO. A2018009).

4.7. Enzymatic activity assays of HsDHODH

Recombinant *Hs*DHODH protein was expressed and purified as described in previous study[19]. The enzyme was diluted into a final concentration of 10 nmol/L with an assay bufier containing 50 mmol/L HEPES at pH 7.7, 150 mmol/L KCl, and Triton X-100 (0.1% *v*/*v*). UQ_0 and DCIP were added into the assay bufier to final concentrations of 100 and 120 μmol/L, respectively. The mixture was transferred into a 96-well plate and incubated for 5 min at room temperature. Compounds were prepared as 10 mmol/L stock solutions in DMSO and further diluted by the assay buffer to prepare working stocks. In the following step, dihydroorotate was added to a final concentration of 500 μmol/L to initiate the reaction. The reaction was monitored by measuring the decrease of DCIP according to its absorption at 600 nm for each 30 s over a period of 6 min. For the determination of the IC_{50}

values, eight to nine difierent concentrations were applied. Each concentration point was tested in triplicate. IC_{50} values were determined by nonlinear regression analysis of logistic concentration (GraphPad Prism software).

4.8. Enzymatic activity assays of PfNDH2

Recombinant *Pf*NDH2 protein was expressed and purified as described in previous study[10]. The enzymatic activity of *Pf*NDH2 proteins was measured spectrophotometrically using NADH and ubiquinone-1 (UQ_1) as substrates. Standard assays were carried out at 25 °C in 1.6 mL of reaction mixture containing 50 mmol/L MOPS buffer, pH 7.0, 150 mmol/L NaCl, 1 mmol/L EDTA, 0.01% Triton-X-100, 200 μmol/L NADH, 100 μmol/L UQ_1, 0.5 nmol/L enzymes, and selected concentrations of inhibitors. Reactions were initiated by the enzyme addition. Progress of the reaction was monitored continuously by following the decrease of signal from NADH at 340 nm, in a Lambda 45 spectrophotometer (PerkinElmer Life Sciences) equipped with a magnetic stirrer in the cuvette holder. Activities were calculated using an NADH extinction of 6220 L/(mol·cm) at 340 nm. IC_{50} values were determined by nonlinear regression analysis of logistic concentration (GraphPad Prism software). In the enzyme kinetic studies, different concentrations of substrates were used (UQ_1: 5, 10, 20, 30, 40, 60, 80, 100 μmol/L. NADH: 10, 20, 30, 50, 75, 100, 200, 600 μmol/L).

4.9. Yeast cytochrome b mutants

The *P. falciparum*-like cytochrome *b* mutants of yeast were generated by side-directed mutagenesis and mitochondrial transformation as described previously[34,41]. They have identical nuclear and mitochondrial genomes with the exception of the mutations introduced in the cytochrome *b* gene.

4.10. Measurement of decylubiquinol-cytochrome c reductase activity

Yeast mitochondria were prepared as before[42]. Briefly, yeast grown in YPGal medium were harvested at mid-log phase. Protoplasts were obtained by enzymatic digestion of the cell wall using zymolyase in an osmotic protection buffer. Mitochondria were then prepared by differential centrifugation following osmotic shock of the protoplasts. Mitochondrial samples were aliquoted and stored at −80 °C. Concentration of cytochrome bc_1 complex in the mitochondrial samples was determined from dithionite-reduced optical spectra, using $\varepsilon = 28.5$ (L/mmol/cm at 562 nm minus 575 nm. Decylubiquinol-cytochrome *c* reductase activities were determined at room temperature by measuring the reduction of cytochrome *c* (final concentration of 20 μmol/L) at 550 nm *versus* 540 nm over 1-min time-course in 10 mmol/L potassium phosphate pH 7, 0.01% (*w/v*) lauryl-maltoside and 1 mmol/L KCN. Mitochondria were added to obtain a final concentration of 6 nmol/L bc_1 complex for WT and 20 nmol/L for the mutants. Activity was initiated by the addition of decylubiquinol (final concentration of 40 μmol/L). Initial rates were measured. Each measurement was repeated at least twice and the values obtained were averaged. Activities are presented as the rate of cytochrome *c* reduction per bc_1 complex per second. The mid-point inhibition concentrations (IC_{50}) were determined by inhibitor titration.

Mitochondria of *P. falciparum* D10 (WT) were isolated using a method published previously[21,43]. Briefly, a large volume of parasite culture (∼2 L) at late trophozoite stages was lysed with saponin (0.05%) and disrupted in a N_2 cavitation chamber (4639 Cell Disruption Vessel, Parr Instrument Company) in an isotonic mitochondrial buffer. The total parasite lysate was spun down at 900×*g* for 6 min to remove large debris, and the cloudy supernatant was passed through a MACS CS column (Miltenyi Biotec) in a Vario MACS magnetic separation apparatus to remove most of the hemozoin. The eluted light-yellow material (nearly hemozoin free) was pelleted at 23,000×*g* for 40 min at 4 °C, and the pellet was re-suspended in buffer and stored at −80 °C. For bc_1 enzymatic measurement, the assay volume was 300 μL, containing mitochondrial proteins (25 μg), 100 μmol/L decylubiquinol (reduced), 75 μmol/L horse heart cytochrome *c* (Sigma−Aldrich), 0.1 mg/mL *n*-docecyl-*β*-D-maltoside, 60 mmol/L HEPES (pH 7.4), 10 mmol/L sodium malonate, 1 mmol/L EDTA, and 2 mmol/L KCN, and was incubated at 35 °C in a stirred cuvette in the CLARITY VF integrating spectrophotometer (OLIS, Bogart, GA). Reduction of oxidized horse heart cytochrome *c* was recorded at 550 nm. A Bio-Rad colorimetric assay was used to measure protein concentrations of all mitochondrial samples. For each compound tested, the maximal activity of ubiquinone-cytochrome *c* reduction (100%) was averaged from five measurements as described above with no addition of any inhibitors. Compounds were dissolved in DMSO and tested in a series of concentrations with each concentration in two or three replicates. Note, *n*-docecyl-*β*-D-maltoside was used as a detergent in the assay.

4.11. Molecular docking, homology modeling and molecular dynamic (MD) simulation

Molecular docking and homology modeling were performed on Schrodinger suites. In the Protein Preparation Wizard, the missing side chains were filled with Prime and all water molecules were removed. The ligands were ionized using Epik at target pH 7.0 ± 2.0 in the LigPrep dialog. Receptor grids were generated by picking the ligands in the proteins or its homologues with similar sizes to the selected ligands. Hydroxyl and thiol groups near the binding pockets were set as rotatable groups to allow rotation. Ligand docking was performed on extra precision (XP) and 20 poses per ligand were written out. The unknown protein structures of *P. falciparum* were built by its corresponding sequence from UniProt with yeast homologues as described in the text under default setting. All the figures were prepared by PyMol.

MD simulation was performed on Desmond[44] by following the above molecular docking and homology modeling of *Pf*b. In the system builder, DPPC (325K) was set as membrane model, which was placed automatically. The solvent model was predefined as TIP3P. NaCl was added as salt at a concentration of 0.15 mol/L. In the minimization step, 100 ps was simulated. Total simulation time was 100 ns, in which the trajectory was recorded every 50 ps and ∼2000 frames were generated under an ensemble class of NPγT. The simulation quality was analyzed in Meastro.

Acknowledgments

We would like to thank Prof. Maojun Yang for supplying *Pf*NDH2 plasmid. This work was supported by the National Natural Science Foundation of China (81622042, 81773567 and 31771455), National Key R&D Program of China (2018YFA0507300, 2018ZX09711001, 2020YFE0202200). Innovation Capacity Building Project of Jiangsu province (BM2020019), and Shanghai Post-doctoral Excellence Program (2020469).

Author contributions

Yu Rao, Lubin Jiang, and Yiqing Yang designed this project. Yu Rao, Lubin Jiang, Hangjun Ke, Brigitte Meunier, and Jing Zhou supervised this project. Yiqing Yang performed molecular docking, homology modeling, cytotoxicity, and solubility assays. Yiqing Yang and Yue Wu performed the chemical synthesis. Tongke Tang and Zhenghui Huang performed most *in vitro* and *in vivo* parasites inhibition assays. Xiaolu Li performed *Pf*NDH2 enzymatic assays. Thomas Michel performed enzymatic assays of wild type and mutant yeast bc_1. Liqin Ling performed assays of yDHOD and its parental parasites. Maruthi Mulaka performed enzymatic assays of *Pf*bc_1. Hongying Gao performed enzymatic assays of *Hs*DHODH. Liguo Wang and Yiqing Yang performed MD simulation. All authors analyzed the data and wrote the manuscript.

Conflicts of interest

The authors declare no competing financial interest.

Appendix A. Supporting information

Supporting information to this article can be found online at https://doi.org/10.1016/j.apsb.2021.05.008.

References

1. World Health Organization. *World malaria report 2020*. Geneva, Switzerland. 2020. Available from: https://www.who.int/publications/i/item/9789240015791.
2. Cheviet T, Lefebvre-Tournier I, Wein S, Peyrottes S. Plasmodium purine metabolism and its inhibition by nucleoside and nucleotide analogues. *J Med Chem* 2019;**62**:8365−91.
3. Blasco B, Leroy D, Fidock DA. Antimalarial drug resistance: linking *Plasmodium falciparu*m parasite biology to the clinic. *Nat Med* 2017;**23**:917−28.
4. Amato R, Pearson RD, Almagro-Garcia J, Amaratunga C, Lim P, Suon S, et al. Origins of the current outbreak of multidrug-resistant malaria in Southeast Asia: a retrospective genetic study. *Lancet Infect Dis* 2018;**18**:337−45.
5. Uwimana A, Legrand E, Stokes BH, Ndikumana JLM, Warsame M, Umulisa N, et al. Emergence and clonal expansion of *in vitro* artemisinin-resistant *Plasmodium falciparum* kelch13 R561H mutant parasites in Rwanda. *Nat Med* 2020;**26**:1602−8.
6. Goodman CD, Buchanan HD, McFadden GI. Is the mitochondrion a good malaria drug target?. *Trends Parasitol* 2017;**33**:185−93.
7. Stocks PA, Barton V, Antoine T, Biagini GA, Ward SA, O'Neill PM. Novel inhibitors of the *Plasmodium falciparum* electron transport chain. *Parasitology* 2014;**141**:50−65.
8. Painter HJ, Morrisey JM, Mather MW, Vaidya AB. Specific role of mitochondrial electron transport in blood-stage *Plasmodium falciparum*. *Nature* 2007;**446**:88−91.
9. Leung SC, Gibbons P, Amewu R, Nixon GL, Pidathala C, Hong WD, et al. Identification, design and biological evaluation of heterocyclic quinolones targeting *Plasmodium falciparum* type II NADH:quinone oxidoreductase (PfNDH2). *J Med Chem* 2012;**55**:1844−57.
10. Yang Y, Yu Y, Li X, Li J, Wu Y, Yu J, et al. Target elucidation by cocrystal structures of NADH-ubiquinone oxidoreductase of *Plasmodium falciparum* (PfNDH2) with small molecule to eliminate drug-resistant malaria. *J Med Chem* 2017;**60**:1994−2005.
11. Petri J, Shimaki Y, Jiao W, Bridges HR, Russell ER, Parker EJ, et al. Structure of the NDH-2–HQNO inhibited complex provides molecular insight into quinone-binding site inhibitors. *Biochim Biophys Acta Bioenerg* 2018;**1859**:482−90.
12. Birth D, Kao WC, Hunte C. Structural analysis of atovaquone-inhibited cytochrome *bc*1 complex reveals the molecular basis of antimalarial drug action. *Nat Commun* 2014;**5**:4029.
13. Lane KD, Mu J, Lu J, Windle ST, Liu A, Sun PD, et al. Selection of *Plasmodium falciparum* cytochrome *B* mutants by putative PfNDH2 inhibitors. *Proc Natl Acad Sci U S A* 2018;**115**:6285−90.
14. Capper MJ, O'Neill PM, Fisher N, Strange RW, Moss D, Ward SA, et al. Antimalarial 4(1*H*)-pyridones bind to the Qi site of cytochrome *bc*1. *Proc Natl Acad Sci U S A* 2015;**112**:755−60.
15. Stickles AM, Smilkstein MJ, Morrisey JM, Li Y, Forquer IP, Kelly JX, et al. Atovaquone and ELQ-300 combination therapy as a novel dual-site cytochrome *bc*1 inhibition strategy for malaria. *Antimicrob Agents Chemother* 2016;**60**:4853−9.
16. David HW, Leung SC, Amporndanai K, Davies J, Priestley RS, Nixon GL, et al. Potent antimalarial 2-pyrazolyl quinolone *bc*1 (Qi) inhibitors with improved drug-like properties. *ACS Med Chem Lett* 2018;**9**:1205−10.
17. Llanos-Cuentas A, Casapia M, Chuquiyauri R, Hinojosa JC, Kerr N, Rosario M, et al. Antimalarial activity of single-dose DSM265, a novel plasmodium dihydroorotate dehydrogenase inhibitor, in patients with uncomplicated *Plasmodium falciparum* or *Plasmodium vivax* malaria infection: a proof-of-concept, open-label, phase 2a study. *Lancet Infect Dis* 2018;**18**:874−83.
18. Mandt REK, Lafuente-Monasterio MJ, Sakata-Kato T, Luth MR, Segura D, Pablos-Tanarro A, et al. *In vitro* selection predicts malaria parasite resistance to dihydroorotate dehydrogenase inhibitors in a mouse infection model. *Sci Transl Med* 2019;**11**:eaav1636.
19. Yang Y, Cao L, Gao H, Wu Y, Wang Y, Fang F, et al. Discovery, optimization, and target identification of novel potent broad-spectrum antiviral inhibitors. *J Med Chem* 2019;**62**:4056−73.
20. Xu M, Zhu J, Diao Y, Zhou H, Ren X, Sun D, et al. Novel selective and potent inhibitors of malaria parasite dihydroorotate dehydrogenase: discovery and optimization of dihydrothiophenone derivatives. *J Med Chem* 2013;**56**:7911−24.
21. Ke H, Ganesan SM, Dass S, Morrisey JM, Pou S, Nilsen A, et al. Mitochondrial type II NADH dehydrogenase of *Plasmodium falciparum* (*Pf*NDH2) is dispensable in the asexual blood stages. *PLoS One* 2019;**14**:e0214023.
22. Paton DG, Childs LM, Itoe MA, Holmdahl IE, Buckee CO, Catteruccia F. Exposing *Anopheles* mosquitoes to antimalarials blocks *Plasmodium parasite* transmission. *Nature* 2019;**567**:239−43.
23. Boysen KE, Matuschewski K. Arrested oocyst maturation in *Plasmodium parasites* lacking type II NADH:ubiquinone dehydrogenase. *J Biol Chem* 2011;**286**:32661−71.
24. Biagini GA, Fisher N, Shone AE, Mubaraki MA, Srivastava A, Hill A, et al. Generation of quinolone antimalarials targeting the *Plasmodium falciparum* mitochondrial respiratory chain for the treatment and prophylaxis of malaria. *Proc Natl Acad Sci U S A* 2012;**109**:8298−303.
25. Song Z, Iorga BI, Mounkoro P, Fisher N, Meunier B. The antimalarial compound ELQ-400 is an unusual inhibitor of the *bc*1 complex, targeting both Qo and Qi sites. *FEBS Lett* 2018;**592**:1346−56.
26. Feng Y, Li W, Li J, Wang J, Ge J, Xu D, et al. Structural insight into the type-II mitochondrial NADH dehydrogenases. *Nature* 2012;**491**:478−82.
27. Leslie CP, Di Fabio R, Bonetti F, Borriello M, Braggio S, Dal Forno G, et al. Novel carbazole derivatives as NPY Y1 antagonists. *Bioorg Med Chem Lett* 2007;**17**:1043−6.
28. Pegoraro S, Duffey M, Otto TD, Wang Y, Rösemann R, Baumgartner R, et al. SC83288 is a clinical development candidate for the treatment of severe malaria. *Nat Commun* 2017;**8**:14193.
29. Mu J, Myers RA, Jiang H, Liu S, Ricklefs S, Waisberg M, et al. *Plasmodium falciparum* genome-wide scans for positive selection, recombination hot spots and resistance to antimalarial drugs. *Nat Genet* 2010;**42**:268−71.
30. Kato N, Comer E, Sakata-Kato T, Sharma A, Sharma M, Maetani M, et al. Diversity-oriented synthesis yields novel multistage antimalarial inhibitors. *Nature* 2016;**538**:344−9.

31. Ke H, Morrisey JM, Ganesan SM, Painter HJ, Mather MW, Vaidya AB. Variation among *Plasmodium falciparum* strains in their reliance on mitochondrial electron transport chain function. *Eukaryot Cell* 2011;**10**:1053−61.
32. Wang J, Zhang CJ, Chia WN, Loh CCY, Li Z, Lee YM, et al. Haem-activated promiscuous targeting of artemisinin in *Plasmodium falciparum*. *Nat Commun* 2015;**6**:10111.
33. Ismail HM, Barton V, Phanchana M, Charoensutthivarakul S, Wong MHL, Hemingway J, et al. Artemisinin activity-based probes identify multiple molecular targets within the asexual stage of the malaria parasites *Plasmodium falciparum* 3D7. *Proc Natl Acad Sci U S A* 2016;**113**:2080−5.
34. Vallières C, Fisher N, Meunier B. Reconstructing the Qo site of *Plasmodium falciparum bc*1 complex in the yeast enzyme. *PLoS One* 2013;**8**:e71726.
35. Song Z, Clain J, Iorga BI, Vallieres C, Laleve A, Fisher N, et al. Interplay between the hinge region of iron sulphur protein and the Qo site in the *bc*1 complex analysis of *Plasmodium*-like mutations in the yeast enzyme. *Biochim Biophys Acta* 2015;**1847**:1487−94.
36. Lencina AM, Franza T, Sullivan MJ, Ulett GC, Ipe DS, Gaudu P, et al. Type 2 NADH dehydrogenase is the only point of entry for electrons into the *Streptococcus agalactiae* respiratory chain and is a potential drug target. *mBio* 2018;**9**:e01034.
37. Lin SS, Gross U, Bohne W. Two internal type II NADH dehydrogenases of *Toxoplasma gondii* are both required for optimal tachyzoite growth. *Mol Microbiol* 2011;**82**:209−21.
38. Sellamuthu S, Singh M, Kumar A, Singh SK. Type-II NADH dehydrogenase (NDH-2): a promising therapeutic target for antitubercular and antibacterial drug discovery. *Expert Opin Ther Targets* 2017;**21**:559−70.
39. Modica-Napolitano JS, Aprille JR. Delocalized lipophilic cations selectively target the mitochondria of carcinoma cells. *Adv Drug Deliv Rev* 2001;**49**:63−70.
40. Shi Y, Lim SK, Liang Q, Iyer SV, Wang HY, Wang Z, et al. Gboxin is an oxidative phosphorylation inhibitor that targets glioblastoma. *Nature* 2019;**567**:341−6.
41. Hill P, Kessl J, Fisher N, Meshnick S, Trumpower BL, Meunier B. Recapitulation in *Saccharomyces cerevisiae* of cytochrome b mutations conferring resistance to atovaquone in *Pneumocystis jiroveci*. *Antimicrob Agents Chemother* 2003;**47**:2725−31.
42. Lemaire C, Dujardin G. Preparation of respiratory chain complexes from *Saccharomyces cerevisiae* wild-type and mutant mitochondria: activity measurement and subunit composition analysis. *Methods Mol Biol* 2008;**432**:65−81.
43. Ke H, Dass S, Morrisey JM, Mather MW, Vaidya AB. The mitochondrial ribosomal protein L13 is critical for the structural and functional integrity of the mitochondrion in *Plasmodium falciparum*. *J Biol Chem* 2018;**293**:8128−37.
44. Bowers KJ, Chow E, Xu H, Dror RO, Eastwood MP, Gregersen BA, et al. Scalable algorithms for molecular dynamics simulations on commodity clusters. In: *Proceedings of the 2006 ACM/IEEE conference on supercomputing, association for computing machinery; 2006, November 11−17; Tampa, FL, USA*. Piscataway: IEEE; 2006.